

# Weyl Semimetals as Hydrogen Evolution Catalysts

Catherine R. Rajamathi, Uttam Gupta, Nitesh Kumar, Hao Yang, Yan Sun, Vicky Süß, Chandra Shekhar, Marcus Schmidt, Horst Blumtritt, Peter Werner, Binghai Yan, Stuart Parkin, Claudia Felser,\* and C. N. R. Rao\*

The search for highly efficient and low-cost catalysts is one of the main driving forces in catalytic chemistry. Current strategies for the catalyst design focus on increasing the number and activity of local catalytic sites, such as the edge sites of molybdenum disulfides in the hydrogen evolution reaction (HER). Here, the study proposes and demonstrates a different principle that goes beyond local site optimization by utilizing topological electronic states to spur catalytic activity. For HER, excellent catalysts have been found among the transition-metal mononictides—NbP, TaP, NbAs, and TaAs—which are recently discovered to be topological Weyl semimetals. Here the study shows that the combination of robust topological surface states and large room temperature carrier mobility, both of which originate from bulk Dirac bands of the Weyl semimetal, is a recipe for high activity HER catalysts. This approach has the potential to go beyond graphene based composite photocatalysts where graphene simply provides a high mobility medium without any active catalytic sites that have been found in these topological materials. Thus, the work provides a guiding principle for the discovery of novel catalysts from the emerging field of topological materials.

Heterogeneous catalysis plays a major role in organic and inorganic chemistry. The high complexity of the catalytic process is a major challenge.<sup>[1–4]</sup> One important catalytic process, of increasing importance, is the harvesting of solar energy to produce hydrogen (H<sub>2</sub>) from water: one of the major challenges in the supply of “green energy.”<sup>[5,6]</sup> Educds, products, and the surface of the catalyst have to be

taken into account in heterogeneous catalysis. Many conventional metals and semiconductors are under investigation as potential catalysts.<sup>[7–9]</sup> A stable supply of itinerant electrons at the surface is important for catalytic processes involving redox reactions. Materials with high mobilities of electrons and holes reduce the probability of recombination of the electron–hole pairs that are created in the redox process. Here we introduce a new concept based on the use of unconventional topological materials as catalysts. While these materials have drawn significant attention from the condensed matter community, their unique properties have not yet been considered by chemists. But the high carrier mobilities that are realized from the linear bands of a Dirac cone and which are thereby a fundamental property of Weyl and Dirac semimetals<sup>[10,11]</sup> suggest that these materials could be excellent

catalysts, as we show here. Moreover, the problem of surface contamination, which is a major bottleneck in the field of catalysis, can be diminished to a great extent in topological materials because of their robust topologically protected surface states.<sup>[12,13]</sup>

The prerequisite to a Weyl semimetal or a topological insulator (TI) is an energy band inversion. Many compounds containing heavy metals show such a band inversion, more commonly referred to, within the chemistry community, as an inert pair effect.<sup>[14]</sup> In a relativistic band structure, band crossing is forbidden such that, in topological insulators, a new bandgap opens, and a surface state with a Dirac cone electronic structure appears. Dirac and Weyl semimetals appear at the borderline between topological and trivial insulators. In a Weyl semimetal, pairs of Dirac cones are formed in the bulk of the material where the number of pairs depends on the detailed symmetry of the particular metal. Weyl semimetals also exhibit unusual surface states with open Fermi arcs. To verify our hypothesis that the new topological materials with superior electronic properties can also be highly efficient in catalysis we have tested them for dye-sensitized hydrogen evolution reaction (HER). In the HER, solar light is absorbed by photon capture systems, such as the dye Eosin Y (EY). The resultant excited electrons can be transferred to the catalyst, on which H<sup>+</sup> in the water is reduced to form H<sub>2</sub>. A schematic representation of the HER process is shown in **Figure 1**.

C. R. Rajamathi, Dr. N. Kumar, Dr. Y. Sun, V. Süß,  
Dr. C. Shekhar, Dr. M. Schmidt,  
Dr. B. Yan, Prof. C. Felser  
Max Planck Institute for Chemical Physics of Solids  
01187 Dresden, Germany  
E-mail: felser@cpfs.mpg.de



U. Gupta, Prof. C. N. R. Rao  
Chemistry and Physics Materials Unit  
New Chemistry Unit and International Centre for Materials Science  
Sheik Saqr Laboratory  
Jawaharlal Nehru Centre for Advanced Scientific Research  
Jakkur P. O., Bangalore 560064, India  
E-mail: cnrrao@ncasr.ac.in

H. Yang, Dr. H. Blumtritt, Dr. P. Werner, Prof. S. Parkin  
Max Planck Institute for Microstructure Physics  
06120 Halle (Saale), Germany

Dr. B. Yan  
Max Planck Institute for the Physics of Complex Systems  
01187 Dresden, Germany

DOI: 10.1002/adma.201606202

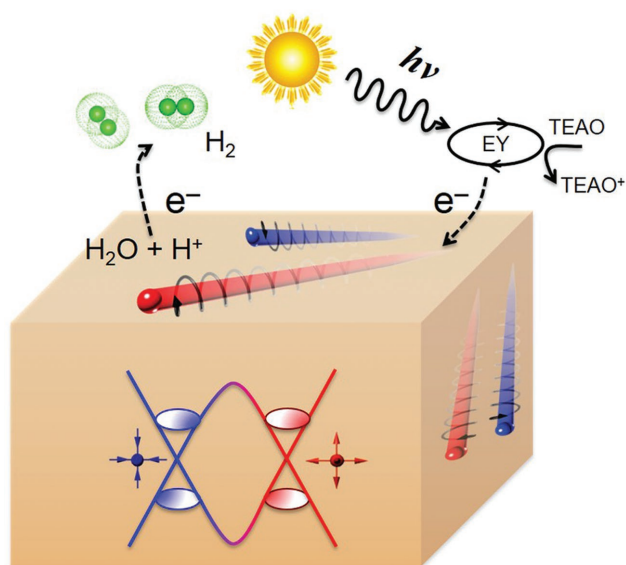


**Figure 1.** Schematic diagram of a TWS for catalyzing the dye-sensitized hydrogen evolution. When light falls upon EY it is excited and, in the presence of the sacrificial agent triethanolamine (TEAO), the dye transfers an electron to the surface of the TWS, leading to charge separation, and, thereby, reducing water to hydrogen. In a TWS the bulk bands are gapped by spin-orbit coupling in momentum space, except for some isolated linear-crossing points, namely, the Weyl points/Dirac points.

Among photocatalysts for hydrogen production, MoS<sub>2</sub> nanoparticles were reported to demonstrate high efficiency to catalyze both photochemical as well as electrochemical HER.<sup>[15–17]</sup> Metallic MoS<sub>2</sub>, either in the form of metallic edges of 2H-MoS<sub>2</sub><sup>[16]</sup> or the metastable metallic 1T polytype,<sup>[16]</sup> is found to be much more active than its semiconducting counterpart. Recent theoretical studies also find that metallic transition metal dichalcogenides (TMDs) are excellent candidates for HER based on considerations, not of their topological properties, but simple free energy calculations.<sup>[18]</sup> However, our proposal goes beyond the concept of metallic versus semiconducting dichalcogenides. We are convinced that the electronic structure of Weyl semimetals favors catalysis. To test whether the metallicity alone is sufficient or rather it is the topology that is at work, we have compared the catalytic performance of several different TMDs for HER: topologically trivial semiconducting 2H-MoTe<sub>2</sub>; topologically trivial metallic 1T-TaS<sub>2</sub>; and topologically nontrivial 1T'-MoTe<sub>2</sub>. Note that Ta has a d<sup>1</sup> configuration (octahedral coordination) in 1T-TaS<sub>2</sub> and Mo has a d<sup>2</sup> configuration (trigonal prismatic coordination) in 2H-MoS<sub>2</sub>, which makes the first system metallic and the latter semiconducting. Additionally, bulk orthorhombic MoTe<sub>2</sub> is type-II Weyl semimetal<sup>[19–23]</sup> while the monolayer<sup>[24]</sup> and few-layers 1T'-MoTe<sub>2</sub> have nontrivial Z<sub>2</sub> topological invariants. We show the calculated band structure of the three TMDs in Figure S1 in the Supporting Information.

HER activities of 1T'-MoTe<sub>2</sub>, 2H-MoTe<sub>2</sub>, and 1T-TaS<sub>2</sub> powdered single crystals are compared in Figure 2a. 1T'-MoTe<sub>2</sub> exhibits a huge H<sub>2</sub> evolution reaching a value of 1294 μmol g<sup>-1</sup> in 6 h. However, semiconducting 2H-MoTe<sub>2</sub> evolves only 28.14 μmol g<sup>-1</sup> in the same period. Surprisingly,

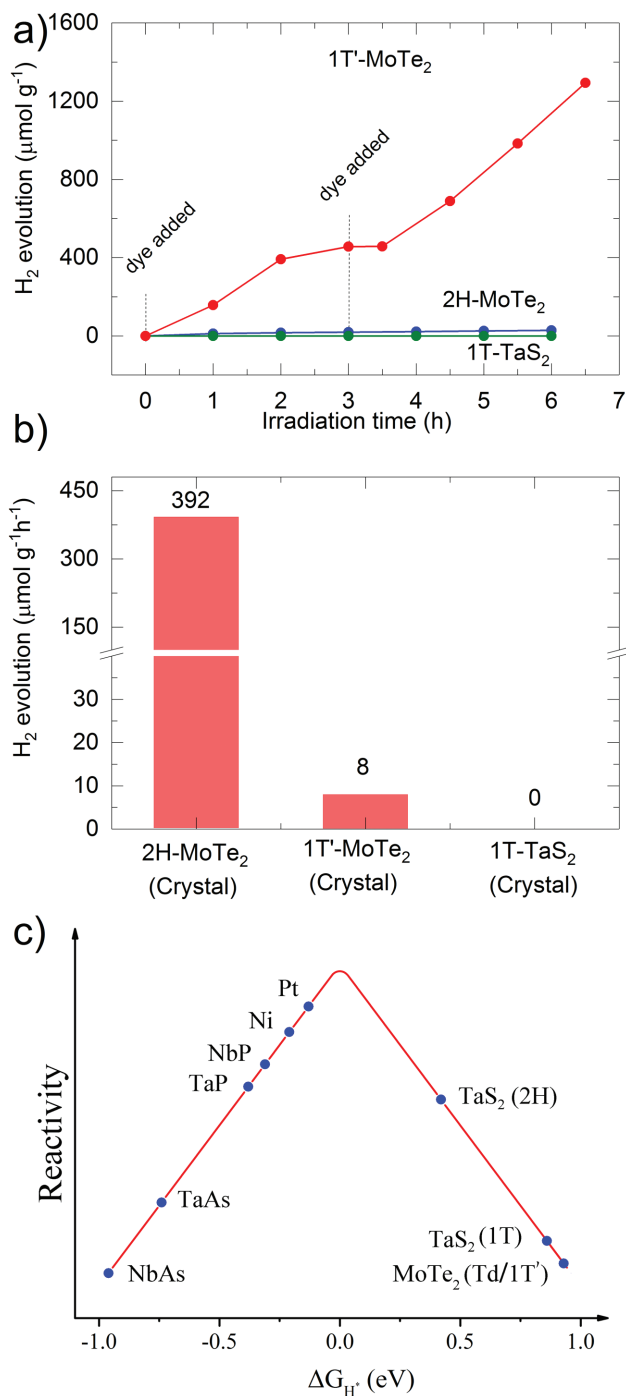


**Figure 2.** Hydrogen evolution in TMDs. a) Comparison of the rate of H<sub>2</sub> evolution using 1T'-MoTe<sub>2</sub>, 2H-MoTe<sub>2</sub>, and 1T-TaS<sub>2</sub>. 1T'-MoTe<sub>2</sub> shows a higher activity compared to its 2H polymorph. b) Histogram of rate of H<sub>2</sub> evolution rate using 1T'-MoTe<sub>2</sub>, 2H-MoTe<sub>2</sub>, and 1T-TaS<sub>2</sub>. c) Predicted relative activities of various HER catalysts following the volcanic scheme as a function of calculated free energy of adsorption of hydrogen on the surface of the catalyst.

metallic 1T-TaS<sub>2</sub> is completely inactive, even though it was predicted to be an active and stable metallic transition metal catalyst based on conventional free energy considerations.<sup>[18]</sup> In Figure 2b, we show a histogram of the rate of H<sub>2</sub> evolution of

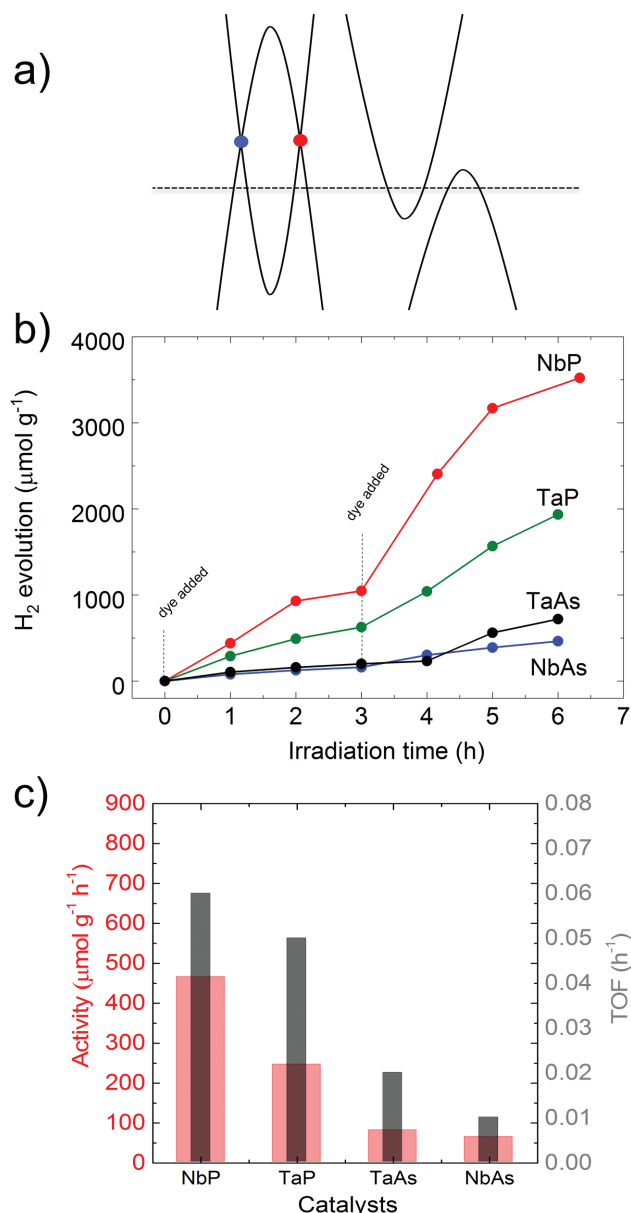


**Figure 3.** Electronic band structure of topological Weyl semimetals and their HER activity. a) Schematic band structure of the transition metal monpnictide TWS family, revealing semimetallic character. Weyl nodes of opposite chiralities are marked with blue and red dots. b) Comparison of hydrogen evolution activity of various TWSs (NbP, TaP, NbAs, and TaAs) powdered single crystals with an intermediate dye addition. c) Histogram of hydrogen evolution rate and TOF, shown on left and right axes, respectively, for all four compounds.

the three compounds where we can clearly see that the topologically nontrivial 1T'-MoTe<sub>2</sub> is the most active catalyst.

The Gibb's free energy ( $\Delta G_{H^*}$ ) of adsorption of hydrogen at the catalyst surface is very often used to predict the activity of an HER catalyst. The closer this value is to zero the better is the performance. The  $\Delta G_{H^*}$  (on abscissa) and the activity (on ordinate) hence make a so-called volcano diagram (Figure 2c). Notwithstanding that both 1T-TaS<sub>2</sub> and 1T'-MoTe<sub>2</sub> are metallic with comparable  $\Delta G_{H^*}$  values, the HER activity of these two compounds

is quite different. As mentioned earlier, 1T-TaS<sub>2</sub> shows almost no HER activity whereas 1T'-MoTe<sub>2</sub> shows a very high activity. Since few-layers 1T'-MoTe<sub>2</sub> rather exhibits topological features in its band structure, this has encouraged us to consider the possible role of topological effects. We consider below the recently discovered Weyl semimetals, NbAs, TaAs, NbP, and TaP.

In a Weyl semimetal, the conduction and valence bands cross each other linearly through nodes (Figure 3a), called the Weyl points, near the Fermi energy. As a 3D analogue of graphene, topological Weyl semimetals (TWSs) are expected to exhibit very high mobility in their charge transport.<sup>[11]</sup> Similar to TIs, TWSs also present robust metallic surface states<sup>[25]</sup> that are stable against defects, impurities, and other surface modifications. Analogous to the role of graphene, in the MoS<sub>2</sub> catalyzed HER, we believe that the highly mobile TWS bulk states help electrons diffuse freely and quickly. Furthermore, the topological surface states may cause the surface to act as stable active planes for catalysis. The first family of TWSs that was experimentally discovered, from direct observations of their topological surface states, was the transition metal monpnictide: NbP, TaP, NbAs, and TaAs.<sup>[26–30]</sup> These materials are semimetals wherein Weyl points are located near the Fermi level with a total of 12 pairs of Weyl nodes in the first Brillouin zone. For this reason, we have investigated the HER activity in these TWS compounds.

The HER activities of NbP, TaP, NbAs, and TaAs were studied over a period of 6 h. Our studies show that all four TWSs are highly HER active (Figure 3c) and NbP, being the lightest among all, performs the best as an HER catalyst with the highest value of H<sub>2</sub> evolved per gram of the catalyst (3520 μmol g<sup>-1</sup>). The compounds can undergo many cycles of HER without activity fading as can be seen in Figure 4b, where we show three cycles of HER in NbP with a comparable catalytic performance each time. Chemical analysis shows no observable changes in chemical composition of our catalysts (Figure S9, Supporting Information) after several HER cycles. We show the activity and turnover frequency (TOF: the number of moles of H<sub>2</sub> evolved per mole of catalyst used) as histograms for all four compounds in Figure 3d. In general, phosphides are better HER catalysts than arsenides. We note that all 4 compounds are WSMs with well-defined and distinct Weyl points and each has very high mobilities from the linearly dispersed bands at the Weyl points, which accounts for their high catalytic activities. We therefore expect that the catalytic HER properties within this series will be determined by the chemical bonding of hydrogen at the surface, which is reflected in the value of  $\Delta G_{H^*}$ . Indeed, we find that their HER activity is correlated with the  $\Delta G_{H^*}$  values for these compounds. NbP has the lowest  $\Delta G_{H^*}$  among all these compounds followed by TaP, TaAs, and NbAs, and TOF also follows a similar trend.

Having investigated the thermodynamic aspects of the catalysts we now focus on the role of kinetics. As we know that the reduction of water occurs at the surface of the catalyst, increasing the surface area of the catalyst should result in increased activity of the catalyst. For this we have selected NbP as an example and compared the activity in single crystals crushed into powder (few μm in size, Figure S9, Supporting Information) and polycrystalline material (150–300 nm in size) obtained by solid state reaction. We encounter a twofold increase in the activity of polycrystals as compared to the single

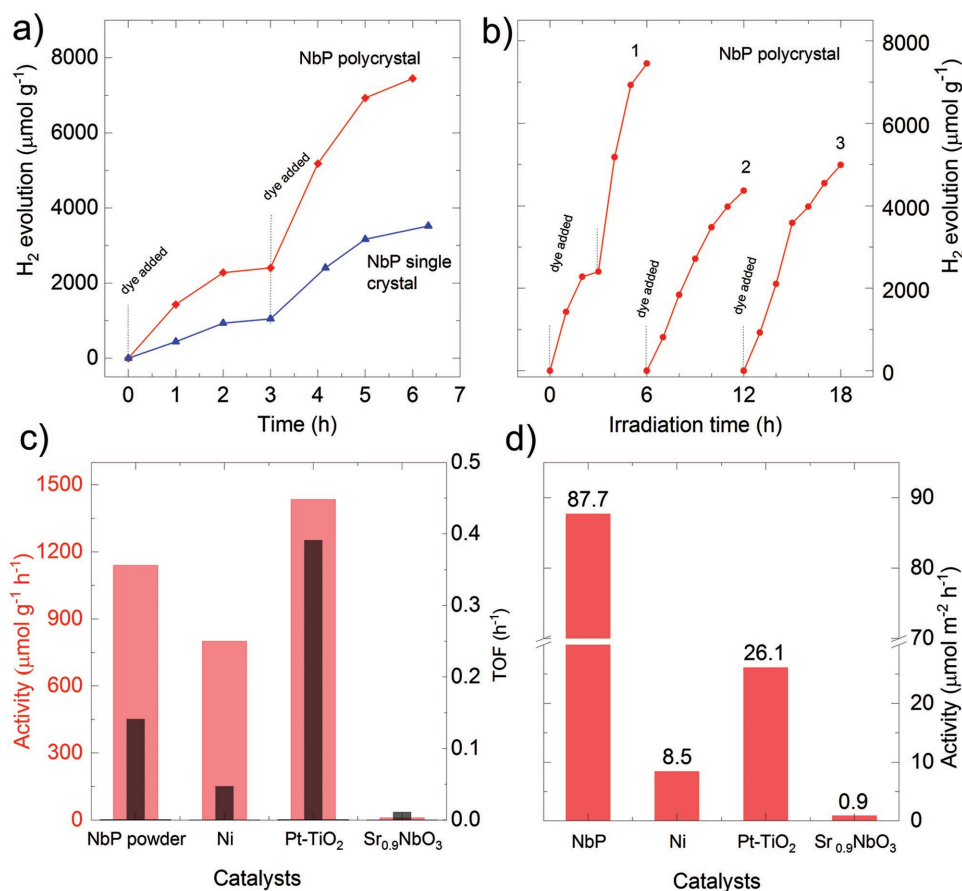


**Figure 4.** H<sub>2</sub> evolution using NbP polycrystalline and single crystalline powders and its comparison with other standard catalysts for HER. a) Comparison of H<sub>2</sub> evolution of NbP in polycrystalline and single crystalline powder form. Polycrystalline powders show higher catalytic activity compared to NbP single crystals. b) Cycling study of polycrystalline NbP powder, indicating the stability of H<sub>2</sub> evolution. c) Histograms for the rate of HER and TOF shown on the left and right axes, respectively, for polycrystalline NbP, Ni metal nanoparticles, Pt-TiO<sub>2</sub> nanoparticles, and Sr<sub>0.9</sub>NbO<sub>3</sub>. d) Corresponding activity scaled to the surface area of the catalysts.

crystals (Figure 4a). The activity in terms of per gram of the catalyst and TOF is comparable to catalysts such as Ni metal nanoparticles<sup>[31]</sup> and highly active platinum decorated TiO<sub>2</sub> nanoparticles,<sup>[32]</sup> under similar experimental conditions (Figure 4c).

In order to draw any conclusive effect of the kinetics we must scale the activity per surface area of the catalyst (Figure 4d). Interestingly, here NbP performs much better than the Ni nanoparticles with an activity that is one order of magnitude higher, despite the fact that the latter has a  $\Delta G_{\text{H}}$  value closer to zero. Moreover, the HER activity of NbP is also higher compared to Pt-TiO<sub>2</sub> (Pt-P25), where the catalytic sites mostly reside at the metallic surface of Pt. The titania nanoparticles used were a mixture of anatase and rutile, and the interfaces of these two polymorphs have been identified as an excellent medium for electron and hole separation. For SrNbO<sub>3</sub>, a well-known visible light absorbing metallic oxide, the activity per unit surface area is two orders of magnitude smaller than for NbP.<sup>[33]</sup>

We now compare the electronic properties of NbP and Ni in order to gain insights into the higher HER activity of NbP compared to Ni, when conventional considerations would suggest the opposite ( $\Delta G_{\text{H}^*}$  is more favorable for Ni than NbP). We note that Ni is highly metallic with a room temperature conductivity

of  $\approx 10^7 \text{ S m}^{-1}$ ; on the other hand, NbP is semimetallic ( $\approx 10^6 \text{ S m}^{-1}$  at room temperature). As the conductivity  $\sigma$  is related to the mobility through the density of charge carriers ( $\sigma = \mu ne$ , where  $\mu$  is the mobility,  $n$  is the carrier density, and  $e$  is the electronic charge), the carriers are much more mobile in NbP as compared to Ni, because of the much smaller carrier density in NbP. The average mobility of NbP is of the order of  $10^3 \text{ cm}^2 \text{ V}^{-1} \text{ s}^{-1}$  as compared to  $\approx 10 \text{ cm}^2 \text{ V}^{-1} \text{ s}^{-1}$  in Ni at room temperature.<sup>[11]</sup> The effect of mobility on the hydrogen evolution reaction has been discussed in the literature, however, has mostly been focused on composite catalysts where graphene is used as a medium to provide for a high mobility of the carriers since graphene has no active catalytic sites.<sup>[34]</sup> Such a material requirement can be overcome in systems where catalytic active sites, as well as high carrier mobility, can be integrated together, for example, the Weyl semimetals studied herein. A large electronic mobility facilitates the rapid transfer of carriers for the catalytic reactions, thereby enhancing the kinetics of HER. It also helps for the rapid separation of electrons and holes. Recent studies on TaAs shows that the bulk Weyl nodes and, therefore, the states close to the projected Fermi arcs on the surfaces, predominantly carry Ta-orbital character.<sup>[35]</sup> This

implies that the As states, as well as the surface states from the trivial bands, are prone to delocalize into the bulk, whereas the Ta states are comparatively more robust on the surface. We, therefore, speculate an important role for transition metal states on the hydrogen evolution activity in our catalysts. Further, we have identified preferred catalytic sites numerically. From the free energy calculations we find that the bridge sites in the Nb/Ta terminated surface are the most active catalytic sites (see Figure S3 in the Supporting Information). In the case of P/As terminated surface, hollow sites are comparatively more active. The details of active catalytic sites for other catalysts are discussed in Figures S4–S6 (Supporting Information).

TWSs serve as excellent candidates for catalysis. We have shown that inherent metallicity alone in a material does not improve catalytic activity, and that the most important factors that one must consider are electronic properties as well as the mobility of carriers. Among the transition metal mononictides, the phosphides are better for HER compared to the arsenides. These catalysts are also robust and therefore can be used long term. They are also durable and have no significant changes in chemical composition after the catalytic procedure. We already observe an improvement in the HER activity with the size reduction when we compare the single crystals and the polycrystalline material. Size reduction plays a more important role in topological materials because the surface states are protected by topology compared to trivial metals. Hence, the effect of disorder will be minimized in topological materials. The activities of TWSs can further be improved significantly by reducing the particle size, for example, by forming them as nanoparticles until the bulk remains metallic.

To conclude, we have shown for two distinct families of Weyl semimetals that their topological electronic structure strongly influences the catalysis of the redox reaction with regard to H<sub>2</sub> evolution from water. We have identified 1T'-MoTe<sub>2</sub>, and NbP and related mononictides as excellent catalysts for the H<sub>2</sub> evolution reaction. Our findings suggest that topological metals or semimetals with high mobilities, robust surface states, and a stable supply of itinerant electrons are promising candidates for catalysis, and thus provide a new route to the discovery of efficient catalysts. In particular, we show that the catalytic activity is several times high per surface area of catalyst compared to well-known catalysts under the same experimental conditions. Moreover, we propose that the chiral surface state of topological materials may even pave the path for asymmetric catalysis.

## Supporting Information

Supporting Information is available from the Wiley Online Library or from the author.

## Acknowledgements

This work was financially supported by ERC Advanced Grant No. (291472) "Idea Heusler."

Received: November 17, 2016

Revised: January 23, 2017

Published online: March 15, 2017

- [1] G. C. Bond, *Heterogeneous Catalysis: Principles and Applications*, Oxford University Press, Oxford, UK **1987**.
- [2] R. Schlögl, *Angew. Chem. Int. Ed.* **2015**, *54*, 3465.
- [3] P. B. Weisz, *Annu. Rev. Phys. Chem.* **1970**, *21*, 175.
- [4] J. K. Norskov, T. Bligaard, J. Rossmeisl, C. H. Christensen, *Nat. Chem.* **2009**, *1*, 37.
- [5] E. Borgarello, J. Kiwi, E. Pelizzetti, M. Visca, M. Gratzel, *Nature* **1981**, *289*, 158.
- [6] X. Wang, K. Maeda, A. Thomas, K. Takane, G. Xin, J. M. Carlsson, K. Domen, M. Antonietti, *Nat. Mater.* **2009**, *8*, 76.
- [7] M. Zeng, Y. Li, *J. Mater. Chem. A* **2015**, *3*, 14942.
- [8] M. G. Walter, E. L. Warren, J. R. McKone, S. W. Boettcher, Q. Mi, E. A. Santori, N. S. Lewis, *Chem. Rev.* **2010**, *110*, 6446.
- [9] X. Zou, Y. Zhang, *Chem. Soc. Rev.* **2015**, *44*, 5148.
- [10] T. Liang, Q. Gibson, M. N. Ali, M. Liu, R. J. Cava, N. P. Ong, *Nat. Mater.* **2015**, *14*, 280.
- [11] C. Shekhar, A. K. Nayak, Y. Sun, M. Schmidt, M. Nicklas, I. Leermakers, U. Zeitler, Y. Skourski, J. Wosnitza, Z. Liu, Y. Chen, W. Schnelle, H. Borrmann, Y. Grin, C. Felser, B. Yan, *Nat. Phys.* **2015**, *11*, 645.
- [12] M. Z. Hasan, C. L. Kane, *Rev. Mod. Phys.* **2010**, *82*, 3045.
- [13] X.-L. Qi, S.-C. Zhang, *Rev. Mod. Phys.* **2011**, *83*, 1057.
- [14] L. M. Schoop, L. Muechler, C. Felser, R. J. Cava, *Inorg. Chem.* **2013**, *52*, 5479.
- [15] H. Li, C. Tsai, A. L. Koh, L. Cai, A. W. Contryman, A. H. Fragapane, J. Zhao, H. S. Han, H. C. Manoharan, F. Abild-Pedersen, J. K. Norskov, X. Zheng, *Nat. Mater.* **2016**, *15*, 48.
- [16] D. Voiry, M. Salehi, R. Silva, T. Fujita, M. Chen, T. Asefa, V. B. Shenoy, G. Eda, M. Chhowalla, *Nano Lett.* **2013**, *13*, 6222.
- [17] U. Maitra, U. Gupta, M. De, R. Datta, A. Govindaraj, C. N. R. Rao, *Angew. Chem. Int. Ed.* **2013**, *52*, 13057.
- [18] C. Tsai, K. Chan, J. K. Norskov, F. Abild-Pedersen, *Surf. Sci.* **2015**, *640*, 133.
- [19] Y. Sun, S.-C. Wu, M. N. Ali, C. Felser, B. Yan, *Phys. Rev. B* **2015**, *92*, 161107.
- [20] Y. Xu, F. Zhang, C. Zhang, *Phys. Rev. Lett.* **2015**, *115*, 265304.
- [21] L. Huang, T. M. McCormick, M. Ochi, Z. Zhao, M.-T. Suzuki, R. Arita, Y. Wu, D. Mou, H. Cao, J. Yan, N. Trivedi, A. Kaminski, *Nat. Mater.* **2016**, *15*, 1155.
- [22] K. Deng, G. Wan, P. Deng, K. Zhang, S. Ding, E. Wang, M. Yan, H. Huang, H. Zhang, Z. Xu, J. Denlinger, A. Fedorov, H. Yang, W. Duan, H. Yao, Y. Wu, S. Fan, H. Zhang, X. Chen, S. Zhou, *Nat. Phys.* **2016**, *12*, 1105.
- [23] J. Jiang, Z. K. Liu, Y. Sun, H. F. Yang, C. R. Rajamathi, Y. P. Qi, L. X. Yang, C. Chen, H. Peng, C. C. Hwang, S. Z. Sun, S. K. Mo, I. Vobornik, J. Fujii, S. S. P. Parkin, C. Felser, B. H. Yan, Y. L. Chen, *Nat. Commun.* **2017**, *8*, 13973.
- [24] X. Qian, J. Liu, L. Fu, J. Li, *Science* **2014**, *346*, 1344.
- [25] X. Wan, A. M. Turner, A. Vishwanath, S. Y. Savrasov, *Phys. Rev. B* **2011**, *83*, 205101.
- [26] H. Weng, C. Fang, Z. Fang, B. A. Bernevig, X. Dai, *Phys. Rev. X* **2015**, *5*, 011029.
- [27] S.-Y. Xu, I. Belopolski, N. Alidoust, M. Neupane, G. Bian, C. Zhang, R. Sankar, G. Chang, Z. Yuan, C.-C. Lee, S.-M. Huang, H. Zheng, J. Ma, D. S. Sanchez, B. Wang, A. Bansil, F. Chou, P. P. Shibayev, H. Lin, S. Jia, M. Z. Hasan, *Science* **2015**, *349*, 613.
- [28] Z. K. Liu, L. X. Yang, Y. Sun, T. Zhang, H. Peng, H. F. Yang, C. Chen, Y. Zhang, Y. F. Guo, D. Prabhakaran, M. Schmidt, Z. Hussain, S. K. Mo, C. Felser, B. Yan, Y. L. Chen, *Nat. Mater.* **2016**, *15*, 27.
- [29] B. Q. Lv, H. M. Weng, B. B. Fu, X. P. Wang, H. Miao, J. Ma, P. Richard, X. C. Huang, L. X. Zhao, G. F. Chen, Z. Fang, X. Dai, T. Qian, H. Ding, *Phys. Rev. X* **2015**, *5*, 031013.

- [30] L. X. Yang, Z. K. Liu, Y. Sun, H. Peng, H. F. Yang, T. Zhang, B. Zhou, Y. Zhang, Y. F. Guo, M. Rahn, D. Prabhakaran, Z. Hussain, S. K. Mo, C. Felser, B. Yan, Y. L. Chen, *Nat. Phys.* **2015**, *11*, 728.
- [31] W. Zhang, Y. Li, X. Zeng, S. Peng, *Sci. Rep.* **2015**, *5*, 10589.
- [32] R. Abe, K. Hara, K. Sayama, K. Domen, H. Arakawa, *J. Photochem. Photobiol., A* **2000**, *137*, 63.
- [33] X. Xu, C. Randorn, P. Efstathiou, J. T. S. Irvine, *Nat. Mater.* **2012**, *11*, 595.
- [34] G. Xie, K. Zhang, B. Guo, Q. Liu, L. Fang, J. R. Gong, *Adv. Mater.* **2013**, *25*, 3820.
- [35] H. Inoue, A. Gyeenis, Z. Wang, J. Li, S. W. Oh, S. Jiang, N. Ni, B. A. Bernevig, A. Yazdani, *Science* **2016**, *351*, 1184.
-